



Title	Neuropeptide Y activates phosphorylation of ERK and STAT3 in stromal vascular cells from brown adipose tissue, but fails to affect thermogenic function of brown adipocytes
Author(s)	Shimada, Kohei; Ohno, Yuta; Okamatsu-Ogura, Yuko; Suzuki, Masahiro; Kamikawa, Akihiro; Terao, Akira; Kimura, Kazuhiro
Citation	Peptides, 34(2), 336-342 https://doi.org/10.1016/j.peptides.2012.02.012
Issue Date	2012-04
Doc URL	http://hdl.handle.net/2115/49225
Type	article (author version)
File Information	Pep34-2_336-342.pdf



[Instructions for use](#)

Neuropeptide Y activates phosphorylation of ERK and STAT3 in stromal vascular cells from brown adipose tissue, but fails to affect thermogenic function of brown adipocytes

Kohei Shimada¹, Yuta Ohno¹, Yuko Okamatsu-Ogura¹, Masahiro Suzuki¹, Akihiro Kamikawa^{1,2}, Akira Terao¹, and Kazuhiro Kimura¹

¹Department of Biomedical Sciences, Graduate School of Veterinary Medicine, Hokkaido University, Sapporo, Japan

²Department of Basic Veterinary Medicine, Obihiro University of Agriculture and Veterinary Medicine, Obihiro, Hokkaido, Japan

Running title: NPY in BAT

Corresponding author: Kazuhiro Kimura, Ph.D.

Department of Biomedical Sciences, Graduate School of Veterinary Medicine, Hokkaido University, Sapporo 060-0818, Japan

Tel. & Fax: +81-11-757-0703, E-mail: k-kimura@vetmed.hokudai.ac.jp

Abstract

The thermogenic function of brown adipose tissue (BAT) is increased by norepinephrine (NE) released from sympathetic nerve endings, but the roles of NPY released along with NE are poorly elucidated. Here, we examined effect of NPY on basal and NE-enhanced thermogenesis in isolated brown adipocytes that express Y1 and Y5 receptor mRNA. Treatment of cells with NPY did not influence the basal and NE-enhanced rates of oxygen consumption and cAMP accumulation. Treatment with NPY also failed to induce ERK (Thr202/Tyr204) phosphorylation in the brown adipocytes. In contrast, treatment with NPY increased ERK phosphorylation in cultured stromal vascular cells from the BAT that express Y1 receptor mRNA. In the latter treatment with NPY also increased STAT3 (Ser727) phosphorylation. These results suggest that NPY mainly acts on stromal vascular cells in BAT and plays roles in the regulation of their gene transcription through ERK and STAT3 pathways, while NPY does not affect the thermogenic function of brown adipocytes.

Key words: BAT, norepinephrine, p44/p42 MAPK, NPY, STAT, thermogenesis

1. Introduction

Acute cold exposure and feeding significantly stimulate thermogenesis in the brown adipose tissue (BAT) [6, 9, 25, 33, 35]. The sympathetic nervous system (SNS) controls this adaptive thermogenesis through the activation of β -adrenergic receptors (β ARs), especially β 3AR. It is well established that β ARs are coupled to the stimulatory G-protein (Gs) and thereby sequentially activate adenylyl cyclase (cAMP formation) and cAMP-dependent protein kinase (PKA). It is also established that active PKA leads to activation of lipolytic enzymes and enhanced expression of the genes encoding uncoupling protein-1 (UCP1). Furthermore, thermogenesis in the BAT is principally dependent on the activation of UCP1, which facilitates proton leakage across the inner mitochondrial membrane to dissipate the electrochemical gradient as heat.

The co-existence of sympathetic and peptidergic innervation has been demonstrated in BAT [5, 11, 23, 28, 38]. Among peptidergic neurotransmitters, neuropeptide Y (NPY) levels in the BAT are significantly decreased and increased by surgical excision of the sympathetic nerves to the BAT and putting an animal into a cold environment, respectively [30]. One study suggested the presence of two separate subpopulations of autonomic nerves in the BAT, that is, one fiber containing both NE and NPY innervates the vascular system, and the other fiber containing only NE innervates the brown adipocytes [5, 6]. Similarly, it is suggested that NPY co-localizes with tyrosine hydroxylase in noradrenergic neurons, but only in the perivascular nerve fiber network [11]. However, other studies showed that NE- and NPY-positive fibers were also found around parenchymal brown adipocytes in mice [38] and rats [23, 28].

NPY exhibits its physiological effects through at least four receptors known as Y1, Y2, Y4, and Y5. It is well established that NPY receptors are coupled to the inhibitory G-protein (Gi) and thereby antagonize β -adrenergic agonist-induced activation of adenylyl cyclase [27, 36]. Moreover, NPY potentiates NE actions via α -adrenoceptor [18, 36, 37], and the potentiation is attributed to the suppression of β -adrenergic action [18]. In the BAT, NPY is suggested to have a vasoconstrictor role at arteriovenous anastomoses [40] and a suppressive role in BAT thermogenesis [30]. However, when treated with NPY and NE in combination for 14 days, rats increase their minimal oxygen consumption by approximately 38% compared with vehicle controls [2]. Similar phenomena are observed in cold acclimated rats [3]. However, direct effects of NPY on BAT thermogenesis have not been elucidated yet.

Therefore, in the present study, we first examined the effects of NPY on brown adipocytes expressing Y1 and Y5 NPY receptors. We also examined the effects of NPY on stromal vascular cells (SVC) expressing Y1 NPY receptor.

2. Materials and methods

2. 1. Materials

Dulbecco's modified Eagle's medium (DMEM) and collagenase were purchased from Wako Pure Chemicals Co. (Osaka, Japan). Fatty acid-free bovine serum albumin (BSA) and isobutylmethylxanthine (IBMX) were purchased from Sigma-Aldrich Fine Chemicals (St. Louis, MO, USA). Fetal calf serum (FCS) was obtained from Trace Scientific Ltd. (Melbourne, Australia). The following antibodies were purchased from Cell Signaling Technology (Beverly, MA, USA): anti-phospho-specific ERK1/2 (p44/42MAPK, Thr-202/Tyr-204) antibody, anti-ERK1/2 antibody, anti-phospho-specific STAT3 (Ser-727) antibody, anti-phospho-specific STAT3 (Tyr-705) antibody, and anti-STAT3 antibody.

2.2. Animals

Experimental procedures and animal care were carried out in accordance with the Guidelines of Animal Care and Use from Hokkaido University, and were approved by the University Committee for the Care and Use of Laboratory Animals. Male 8-week-old C57BL/6J mice were obtained from Nihon SLC (Shizuoka, Japan), housed under specific pathogen-free conditions at 24°C with a 12 h:12 h light:dark cycle, and given food and water *ad libitum*.

2.3. Isolation of brown adipocytes and stromal vascular cells (SVC)

Mice were anesthetized with an intraperitoneal injection of pentobarbital (50 mg/Kg). The whole body was perfused first with Ca²⁺- and Mg²⁺-free PBS and then with Krebs-Ringer bicarbonate HEPES buffer (KRBH, pH 7.4) containing collagenase (1

mg/ml), through a cannula inserted into the left ventricle with a drain from the right atrium in an open-chest procedure. Interscapular BAT was then rapidly removed and placed in PBS. After careful removal of extraneous tissue, the BAT of two mice was transferred in KRBH containing fatty acid-free BSA (10 mg/ml), 2.5 mM glucose, and collagenase (1 mg/ml), minced well, and incubated for 30 minutes at 37 °C with shaking at 90 cycles/min. The cell suspension was passed through a 200- μ m nylon filter and the filtrate was centrifuged at 200 g for 1 min at room temperature. The floating cells were collected as brown adipocytes, and washed 3 times with KRBH to eliminate collagenase. The cells were diluted to a density of $3\text{-}5 \times 10^5$ cells/ml for BAT with the assay buffer [KRBH containing fatty acid-free BSA (40 mg/ml) and 2.7 mM glucose]. The cell suspensions were kept for 1 h at room temperature before analysis. The remainder after the collection of adipocytes was centrifuged at 1,200 g for 10 min at room temperature. The supernatant was removed and the pellet was suspended and cultured in DMEM containing 10% FCS in collagen-coated dishes (Iwaki-Asahi Techno Glass, Chiba, Japan), and the media were changed every 2 days. Cells between the first and second passages were used for the experiments as stromal vascular cells (SVC).

2.4. Measurement of oxygen consumption in isolated brown adipocytes

Oxygen consumption of isolated adipocytes was measured polarographically with a Clark-style oxygen electrode in a water-jacketed Perspex chamber at 37 °C [29]. The cell suspension (200 μ l) was added to a magnetically stirred chamber set with a thermostat at 37°C and was adjusted to a final volume of 1 ml with the assay buffer. The chamber was closed, and the cells were incubated for 5 min to determine the basal respiratory rate. NE and/or NPY were then injected with a Hamilton syringe through a

small hole in the cover of the chamber. Oxygen concentration in the chamber was monitored for 15 min. Oxygen consumption rates were calculated using a computer program (782 System, Strathkelvin Instruments, Glasgow, Scotland, UK).

2.5. cAMP accumulation in isolated brown adipocytes

Isolated adipocytes (3×10^5 cells) were incubated in 0.9 ml of the assay buffer containing 0.5 mM IBMX (a phosphodiesterase inhibitor), and stimulated with NE (1 μ M) and/or NPY (0.1 μ M) for 10 min. HCl (0.1 ml, 1N) was then added and samples were kept on ice for 10 min before centrifugation at $15,000\times g$ for 15 min at 4 °C. The cAMP content in the supernatant was then measured using a cyclic AMP Assay kit (Enzo Life Sciences International, Inc., Plymouth Meeting, PA, USA), according to the protocol provided.

2.6. ERK activation in isolated brown adipocytes

Isolated adipocytes (5×10^4 cells) were incubated in 0.1 ml KRBH, and stimulated with NE (1 μ M) and/or NPY (0.1 μ M) for 10 min. HCl (10 μ l, 1N) was then added and samples were kept on ice for 10 min before adding chloroform/methanol (1:2, 0.5 ml). The solution was centrifuged at $15,000\times g$ for 1 min at 4 °C, and the resultant pellet was washed once with chloroform/methanol and solubilized in a sample buffer for SDS-PAGE.

2.7. Western blotting

Aliquots of cellular protein as described above (20 μ g) were separated by SDS-PAGE and the proteins were transferred onto PVDF membranes (Immobilon; Millipore,

Bedford, MA, USA). The membranes were incubated in a blocking buffer [20 mM Tris/HCl (pH7.5)/150 mM NaCl] containing 0.1% Tween 20 and 1% skimmed milk, and then in the buffer containing a primary antibody. The bound primary antibody was visualized using horseradish peroxidase-linked goat anti-rabbit IgG (Zymed Laboratories, South San Francisco, CA, USA) and chemiluminescent HRP Substrate (Millipore) according to the manufacturer's instructions. The intensity of chemiluminescence for the corresponding bands was analyzed using Image J, a public-domain image-processing and analysis program.

2.8. Cell culture and treatments

SVC were cultured onto 100 mm dishes in DMEM supplemented with 10% fetal bovine serum in 5% CO₂ in humidified air at 37°C. After cells were grown to confluence, they were cultured in a serum-free medium for 24 h to render them quiescent. The cells were then treated with NPY and vehicle (PBS) for 10 min at 37°C. Subsequently, the cells were washed once with buffer [50 mM Hepes (pH7.5), 150 mM NaCl, 5 mM EDTA, 10 mM sodium pyrophosphate, 2 mM NaVO₃, protease inhibitor mixture (Complete; Roche Diagnostics, GmbH, Germany)], then lysed with the buffer containing 1% Nonidet P-40. The lysate was kept on ice for 30 min and centrifuged at 15,000g for 15 min at 4°C. The resulting supernatant was stored at -30°C. Proteins were determined by the Lowry method using BSA as a standard [26]. When treated, PD98059 (an ERK kinase inhibitor; EMD Biosciences, Inc., La Jolla, CA, USA) was added to the cultured cells 2 h before NPY stimulation. Aliquots of the cell lysate were analyzed by Western blotting.

2.9. Cell proliferation assay

SVC (5×10^3 cells) were cultured in 96-well plates with DMEM containing 1% FCS and increasing concentrations of NPY for 72 h. Then, the number of cells was assessed using Cell Counting Kit-8 (DOJINDO, Kumamoto, Japan).

2.10. mRNA analysis

Total cellular RNA was isolated from isolated adipocytes, cultured cells and mouse tissues by the guanidine-isothiocyanate method using RNAiso reagent (Takara Bio, Shiga, Japan). First, 2 μ g of total RNA was mixed with DNaseI reaction buffer [DNaseI (Roche), 40 mM Tris-HCl (pH7.2), 6 mM MgCl₂, ribonuclease inhibitor (Takara)]. The reaction was carried out at 37 °C for 30 min, and terminated at 95 °C for 5 min. Then, single-strand cDNA was synthesized using 100 units of Moloney murine leukemia virus reverse transcriptase (Invitrogen Co., Carlsbad, CA, USA), 50 pmol poly(dT) primer, and 20 nmol dNTP in a total volume of 20 μ l at 37 °C for 1 h. The reaction was terminated at 95 °C for 5 min.

The expression of mRNA was analyzed by conventional PCR or real-time PCR using the cDNA as a template. PCR amplification was performed with 2.5 units Taq polymerase (Ampliqon, Herlev, Denmark), 3 mM MgCl₂, and 50 pmol forward and reverse primers specific to the respective genes in a total volume of 25 μ l. Denaturation and annealing were performed at 94 °C and 58 °C for 30 sec, respectively, while extension was performed at 72 °C for 60 sec. The primers used are summarized in Table 1. The PCR products were analyzed by electrophoresis in 2% agarose gel and stained with ethidium bromide. The PCR products were subcloned into the pGEM-T Easy

vector (Promega, Madison, WI, USA). After the nucleotide sequence of each cDNA was confirmed, the cDNA were used as standards for real-time PCR. To quantify *Egr-1* gene expression levels, real-time PCR was performed with a fluorescence thermal cycler (Light Cycler System, Roche) using 0.5 mM of each primer (Table 1). The fluorescence of SYBR Green (Qiagen, Hilden, Germany) at 530 nm was recorded at the end of the extension phase and analyzed using the Light Cycler Software (Version 3). The level of mouse glyceraldehyde-3-phosphate dehydrogenase (*Gapdh*) mRNA was also determined as an internal control.

2.11. Statistical analysis

The results are expressed as means \pm SD. Statistical analyses were performed using ANOVA and Bonferroni's test, with $p < 0.05$ being considered statistically significant.

3. Results

Brown adipocytes and stromal vascular cells (SVC) were isolated from the mouse interscapular BAT. RT-PCR analyses revealed that the former expressed Y1 and Y5, but not Y2, types of NPY receptors, while the latter mainly expressed Y1 NPY receptor (Fig. 1). To evaluate the effects of NPY on brown adipocytes, we measured *in vitro* oxygen consumption rate of isolated adipocytes as an indicator of thermogenic function. Oxygen consumption rate was 2.9 ± 0.7 nmol O₂/min/10⁵ cells before stimulation and increased to 15.0 ± 4.3 nmol O₂/min/10⁵ cells after stimulation with NE at 1 μM and 10 μM (Fig. 2A). When stimulated with NPY (0.01-1 μM), oxygen consumption rate did not change from the basal rate (Fig. 2B). When simultaneously stimulated with NPY (0.1 μM) and NE (1 μM), oxygen consumption rate did not change from the NE-enhanced rate (Fig. 2C). NPY also failed to modify the NE-enhanced rate even at the sub-maximal concentration of NE used (0.1 μM, Fig. 2D). Next, we measured cAMP formation of isolated adipocytes in the presence of a phosphodiesterase inhibitor. cAMP accumulation was 15.9 ± 11.0 pmol/10⁵ cells before stimulation and increased to 125.8 ± 1.9 pmol/10⁵ cells after stimulation with NE at 1 μM (Fig. 3A). When stimulated with NPY (0.1 μM) in the absence or presence of NE stimulation, cAMP accumulation did not change from the basal or NE-increased level, respectively (Fig. 3A). Furthermore, when examining NPY-induced ERK signaling pathway as reported previously [14, 16, 19, 34], NPY failed to activate activity-related site-specific phosphorylation of ERK (Thr202/Tyr204) in isolated adipocytes while NE stimulated it (Fig. 3B). Therefore, it is unlikely that NPY controls basal and NE-regulated thermogenesis, although mRNAs of NPY receptors were expressed.

To evaluate the effects of NPY on SVC, we examined whether NPY induced

ERK phosphorylation. As shown in Figure 4, treatment of cells with NPY (30 nM and 100 nM) induced the phosphorylation, indicating that functional NPY receptor was present in SVC. We further examined STAT3 phosphorylation at Ser727 and Tyr705, as the serine residue of STAT3 is known to be a downstream target of the ERK pathway [15, 17, 22, 24, 39]. NPY treatment at the concentration of 30 nM or higher induced the Ser phosphorylation, but not the Tyr phosphorylation (Fig. 5). In time course analyses, NPY induced ERK phosphorylation in 3 min after the stimulation, which ended at 30 min, while NPY induced and ceased STAT3 phosphorylation at Ser727 at 10 min and 30 min after the stimulation, respectively (Figs. 4 and 5). Prior treatment of PD98059, an ERK kinase (MEK) inhibitor, suppressed both phosphorylation of ERK and STAT3 at Ser727 (Fig. 6). Moreover, treatment of SVC with NPY increased the immediate early gene, *Egr-1* (early growth response 1, a STAT3-responsive gene) mRNA expression at 1 h after the stimulation, and prior treatment of PD98059 suppressed the expression (Fig. 7).

To evaluate the role of NPY in the regulation of SVC function, we examined whether NPY induced cell growth since NPY promotes proliferation of adipocyte precursor cells in visceral adipose tissue [42]. In contrast to the report, NPY failed to stimulate cell growth of stromal vascular cells of BAT (Fig. 8).

Discussion

In the present study, we have demonstrated for the first time that NPY fails to affect the basal and NE-enhanced cAMP production, ERK phosphorylation and oxygen consumption of brown adipocytes *in vitro*. These phenomena are inconsistent with the previous findings that NPY has a suppressive role in the BAT thermogenesis when given intraperitoneally [30]. As central activation and suppression of NPY neuron decrease and promote BAT function, respectively [6, 8, 21], this inconsistency may be explained by the assumption that intraperitoneally administered NPY leads to activation of central NPY neurons. However, central action induced by peripheral NPY remains to be elucidated. Our observation also conflicts with the reports showing that NPY antagonizes β -adrenergic agonist-induced activation of adenylyl cyclase [27, 36]. As mRNAs of Y1 and Y5 receptors coupled to Gi protein were detected in brown adipocytes, suppression of cAMP production and prevention of increase in oxygen consumption were simply expected. However, the failure of NPY to modulate the cAMP production, oxygen consumption and also ERK activation suggests that functional NPY receptors are lacking in brown adipocytes. Therefore, it is unlikely that NPY directly controls basal and NE-regulated thermogenesis in a short period of time, even if some sympathetic nerves carrying both NE and NPY innervate brown adipocytes [23, 28, 38].

In contrast to brown adipocytes, we have demonstrated that NPY activates ERK phosphorylation in stromal vascular cells (SVC) from the BAT. NPY has been shown to activate ERK pathway in a variety of cells, possibly leading to cell proliferation of neuronal precursor cells [14, 16] and progression of cancer [34]. Moreover, Yang et al. show that NPY promotes ERK-dependent proliferation of adipocyte precursor cells

from the white adipose tissue [42]. We also observed NPY induction of *Egr-1* gene, a transcription factor involved in cell proliferation and in the regulation of apoptosis [12, 13]. It is thus assumed that NPY released from sympathetic nerve terminal stimulates proliferation of SVC, resulting in hyperplasia of the BAT, which occurs in response to physiological stimuli such as cold exposure [20]. However, NPY failed to promote proliferation of SVC from the BAT. The difference in cellular response to NPY in adipocyte precursor cells between the white and brown adipose tissues may be simply due to the different characteristics of these cells which expressing different genes.

STAT3 is a transcription factor and activated upon phosphorylation of the tyrosine residue at amino acid 705 by Janus-activated kinase (JAK) upon the stimulation of a variety of cytokine receptors [4]. In cultured SVC, STAT3 at Tyr705 was constitutively phosphorylated by unknown mechanisms. As transformation of fibroblasts by viral Src induces constitutive activation of STAT3 at Tyr705 [4, 7], non-receptor tyrosine kinases such as cellular Src (c-Src) might be involved in the constitutive activation of STAT3 in the cells used. Under these conditions, we have demonstrated for the first time that NPY induced phosphorylation of STAT3 at Ser727. It is likely that ERK is a STAT3 kinase, since ERK activation preceded phosphorylation of STAT3 at Ser727 and the MEK inhibitor abrogated the phosphorylation of both ERK and STAT3 in SVC, as reported previously [15, 17, 22, 24, 39].

Tyrosine phosphorylation of STAT3 plays pivotal roles in its nuclear translocation and transcriptional activating function [4, 31], but it is a fact that the Y705F mutant of STAT3, which cannot be phosphorylated on tyrosine, also activates some gene expression [41]. There are also conflicting reports regarding the significance of the serine phosphorylation of STAT3 in its transcriptional activating function [10]. That is,

STAT3 phosphorylation at Ser727 has been shown to reduce and increase the transcriptional potential of STAT3. In either case, our result that NPY enhanced a STAT3-responsible gene (*Egr-1*) expression in a MEK-dependent manner suggests the possibility that NPY modulates ERK- and STAT3-dependent transcription via its Ser727 phosphorylation. In addition, NPY is known to control various genes including neuropeptide precursors [1, 32]. Therefore, STAT3 may be important in NPY-dependent transcriptional regulation.

In summary, the present results suggest that NPY acts on SVC in BAT and plays roles in the regulation of their gene transcription through ERK and STAT3 pathways, while NPY does not affect the thermogenic function of brown adipocytes.

Acknowledgements

This work was supported by grants from the Japan Society for the Promotion of Science (JSPS) to K.K. The work was also supported by JSPS Research Fellowships for Young Scientists to K.S.

References

- [1] Abe K, Kuo L, Zukowska Z. Neuropeptide Y is a mediator of chronic vascular and metabolic maladaptations to stress and hypernutrition. *Exp Biol Med* 2010; 235: 1179-1184.
- [2] Al-Arabi A, Andrews JF. Synergistic action by neuropeptide Y (NPY) and norepinephrine (NE) on food intake, metabolic rate, and brown adipose tissue (BAT) causes remarkable weight loss in the obese (*fa/fa*) Zucker rat. *Biomed Sci Instrum* 1997; 33: 216-225.
- [3] Al-Arabi A, Andrews JF. The synergistic effect of sustained administration of neuropeptide y and norepinephrine on the brown fat metabolic activity in cold acclimated obese rats. *Biomed Sci Instrum*. 2009; 45: 54-58.
- [4] Benekli M, Baer MR, Baumann H, Wetzler M. Signal transducer and activator of transcription proteins in leukemias. *Blood* 2003; 101: 2940-2954.
- [5] Cannon B, Nedergaard IT, Lundberg JM, Hokfelt T, Terenius L, Goldstein M. Neuropeptide Tyrosine (NPY) is co-stored with noradrenaline in vascular but not in parenchymal sympathetic nerves of brown adipose tissue. *Exp Cell Res* 1986; 164: 546-550.
- [6] Cannon B, Nedergaard J. Brown adipose tissue: function and physiological significance. *Physiol Rev* 2004; 84: 277–359.
- [7] Cao X, Tay A, Guy GR, Tan YH. Activation and association of Stat3 with Src in v-Src-transformed cell lines. *Mol Cell Biol* 1996; 16: 1595–1603.
- [8] Chao P-T, Yang L, Aja S, Moran TH, Bl S. Knockdown of NPY expression in the dorsomedial hypothalamus promotes development of brown adipocytes and prevents diet-induced obesity. *Cell Metab* 2011; 13: 573-583.

- [9] Collins S, Yehuda-Shnaidman E, Wang H. Positive and negative control of Ucp1 gene transcription and the role of β -adrenergic signaling networks. *Int J Obes* 2010; 34 Suppl 1: S28-S33.
- [10] Decker T, Kovarik P. Serine phosphorylation of STATs. *Oncogene* 2000; 19: 2628–2637.
- [11] De Matteis R, Ricquier D, Cinti S. TH-, NPY-, SP-, and CGRP-immunoreactive nerves in interscapular brown adipose tissue of adult rats acclimated at different temperatures: an immunohistochemical study. *J Neurocytol* 1988; 27: 877-886.
- [12] Gitenay D, Baron VT. Is EGR1 a potential target for prostate cancer therapy? *Future Oncol* 2009; 5: 993-1003.
- [13] Gómez-Martín D, Díaz-Zamudio M, Galindo-Campos M, Alcocer-Varela J. Early growth response transcription factors and the modulation of immune response: implications towards autoimmunity. *Autoimmun Rev* 2010; 9: 454-458.
- [14] Hansel DE, Eipper BA, Ronnett GV. Neuropeptide Y functions as a neuroproliferative factor. *Nature* 2001; 410: 940-944.
- [15] Haq R, Halupa A, Beattie BK, Mason JM, Zanke BW, Barber DL. Regulation of erythropoietin-induced STAT serine phosphorylation by distinct mitogen-activated protein kinases. *J Biol Chem* 2002; 277: 17359-17366.
- [16] Howell OW, Doyle K, Goodman JH, Scharfman HE, Herzog H, Pringle A, Beck-Sickinger AG, Gray WP. Neuropeptide Y stimulates neuronal precursor proliferation in the post-natal and adult dentate gyrus. *J Neurochem* 2005; 93: 560-570.
- [17] Kanai M, Konda Y, Nakajima T, Izumi Y, Kanda N, Nanakin A, Kubohara Y, Chiba T. Differentiation-inducing factor-1 (DIF-1) inhibits STAT3 activity involved in gastric

- cancer cell proliferation via MEK-ERK-dependent pathway. *Oncogene* 2003; 22: 548-554.
- [18] Kanevskij M, Taimor G, Schäfer M, Piper HM, Schlüter KD. Neuropeptide Y modifies the hypertrophic response of adult ventricular cardiomyocytes to norepinephrine. *Cardiovasc Res* 2002; 53: 879-887.
- [19] Keffel S, Schmidt M, Bischoff A, Michel MC. Neuropeptide-Y stimulation of extracellular signal-regulated kinases in human erythroleukemia cells. *J Pharmacol Exp Ther* 1999; 291: 1172-1178.
- [20] Klingenspor M. Cold-induced recruitment of brown adipose tissue thermogenesis. *Exp Physiol* 2003; 88: 141-148.
- [21] Kotz CM, Wang CF, Briggs JE, Levine AS, Billington CJ. Effect of NPY in the hypothalamic paraventricular nucleus on uncoupling proteins 1, 2, and 3 in the rat. *Am J Physiol Regul Integr Comp Physiol* 2000; 278: R494-R498.
- [22] Lee HK, Jung J, Lee SH, Seo SY, Suh DJ, Park HT. Extracellular signal-regulated kinase activation is required for serine 727 phosphorylation of STAT3 in Schwann cells *in vitro* and *in vivo*. *Korean J Physiol Pharmacol* 2009; 13: 161-168.
- [23] Lever JD, Mukherjee S, Norman D, Symons D, Jung RT. Neuropeptide and noradrenaline distributions in rat interscapular brown fat and its intact and obstructed nerves of supply. *J Auton Nerv Syst* 1988; 25: 15-25.
- [24] Lin WF, Chen CJ, Chang YJ, Chen SL, Chiu IM, Chen L. SH2B1beta enhances fibroblast growth factor 1 (FGF1)-induced neurite outgrowth through MEK-ERK1/2-STAT3-Egr1 pathway. *Cell Signal* 2009; 21: 1060-1072.
- [25] Lowell BB, Spiegelman BM. Towards a molecular understanding of adaptive thermogenesis. *Nature* 2000; 404: 652-660.

- [26] Lowry OH, Rosebrough NJ, Farr AL, Randall RJ. Protein measurement with the folin phenol reagent. *J Biol Chem* 1951; 193: 265-275.
- [27] Miller BC, Schluter KD, Zhou XJ, McDermott BJ, Piper HM. Neuropeptide Y stimulates hypertrophy of adult ventricular cardiomyocytes. *Am J Physiol Cell Physiol* 1994; 266: C1271–C1277.
- [28] Norman D, Mukherjee S, Symons D, Jung RT, Lever JD. Neuropeptides in interscapular and perirenal brown adipose tissue in the rat: a plurality of innervation. *J Neurocytol* 1988; 17: 305-311.
- [29] Omachi A, Matsushita Y, Kimura K, Saito M. Role of uncoupling protein 1 in the anti-obesity effect of β 3-adrenergic agonist in the dog. *Res Vet Sci* 2008; 85: 214-219.
- [30] Rebagliati I, Ricci C, Zaninovic A, Tang F. Neuropeptide Y suppressed the T3-induced rise in brown fat mitochondrial respiration in hypothyroid rats. *Endocr Res* 2001; 27: 367-375.
- [31] Reich NC, Liu L. Tracking STAT nuclear traffic. *Nat Rev Immunol* 2006; 6: 602-612.
- [32] Robidoux J, Simoneau L, St-Pierre S, Masse A, Lafond J. Characterization of neuropeptide Y-mediated corticotropin-releasing factor synthesis and release from human placental trophoblasts. *Endocrinology* 2000; 141: 2795-2804.
- [33] Robidoux J, Martin TL, Collins S. Beta-adrenergic receptors and regulation of energy expenditure: a family affair. *Annu Rev Pharmacol Toxicol* 2004; 44: 297–323.
- [34] Ruscica M, Dozio E, Motta M, Magni P. Role of neuropeptide Y and its receptors in the progression of endocrine-related cancer. *Peptides* 2007; 28: 426-434.
- [35] Saely CH, Geiger K, Drexel H. Brown versus white adipose tissue: a mini-review. *Gerontology* 2010; DOI: 10.1159/000321319

- [36] Silva AP, Cavadas C, Grouzmann E. Neuropeptide Y and its receptors as potential therapeutic drug targets. *Clin Chim Acta* 2002; 326: 3-25.
- [37] Wahlestedt C, Edvinsson L, Ekblad E, Hakanson R. Neuropeptide Y potentiated noradrenaline-evoked vasoconstriction: mode of action. *J Pharmacol Exp Ther* 1985; 234: 735–741.
- [38] Watanabe J, Mishiro K, Amatsu T, Kanamura S. Absence of paravascular nerve projection and cross-innervation in interscapular brown adipose tissues of mice. *J Auton Nerv Syst* 1994; 49: 269-276.
- [39] Wierenga AT, Vogelzang I, Eggen BJ, Vellenga E. Erythropoietin-induced serine 727 phosphorylation of STAT3 in erythroid cells is mediated by a MEK-, ERK-, and MSK1-dependent pathway. *Exp Hematol* 2003; 31: 398-405.
- [40] Woods AJ, Stock M. Inhibition of brown fat activity during hypothalamic stimulation in the rat. *Am J Physiol* 1996; 270: R605–R613.
- [41] Yang J, Stark GR. Roles of unphosphorylated STATs in signaling. *Cell Res* 2008; 18: 443-451.
- [42] Yang K, Guan H, Arany E, Hill DJ, Cao X. Neuropeptide Y is produced in visceral adipose tissue and promotes proliferation of adipocyte precursor cells via the Y1 receptor. *FASEB J.* 2008; 22: 2452-2464.

Table 1. Primer list

Gene (Accession No.)	Forward primer sequence Reverse primer sequence (PCR product size)
Npy1r (NM_010934)	5`- TCA ACA GAG GTG AAC AGA CG -3` 5`- TCA ATG CCA GGT TTC CAG AG -3` (+69 to + 429, 361 bps)
Npy2r (NM_008731)	5`- ATG GGC CAG GGC ACA CTA CT -3` 5`- GGG TGT TCA CCA AAA GAT CC -3` (+339 to + 581, 243 bps)
Npy5r (NM_016708)	5`- CAT GCC ATT CCT TCA GTG TG -3` 5`- TCT GGA ACG GTT AGG TGC TT -3` (+550 to + 1140, 591 bps)
egr1 (NM_007913)	5'- TGG CCT GAA CCC CTT TTC AG -3' 5'- GTA GAT GGG ACT GCT GTC GT -3' (+721 to + 885, 165 bps)
Gapdh (NM_008084)	5'- GAA GGT CGG TGT GAA CGG ATT -3' 5'- AAG ACA CCA GTA GAC TCC ACG A -3' (+56 to + 349, 294 bps)

Figure legends

Fig. 1 Expression of NPY receptors.

Conventional RT-PCR was performed on the mRNA obtained from mouse brain, stromal vascular cells (SVC) and brown adipocytes (BA) isolated from mouse interscapular BAT in order to detect expression of NPY receptors, Y1, Y2, and Y5.

Fig. 2 Norepinephrine (NE) increased oxygen consumption of isolated brown adipocytes, but NPY failed to modify basal and NE-enhanced oxygen consumption.

Oxygen consumption by brown adipocytes was monitored *in vitro* for 20 min, and increasing concentrations of NE (A) and NPY (B) and their combination (C, D) were added at 5 min after the onset of the monitoring (arrows). Data are mean \pm SD of values from 3 independent experiments.

Fig. 3 Norepinephrine (NE) increased cAMP formation and ERK phosphorylation in isolated brown adipocytes, but NPY failed to modify basal and NE-induced cAMP formation and ERK phosphorylation. Brown adipocytes were stimulated with NE (1 μ M) and/or NPY (100 nM) for 10 min in the presence (A) and absence (B) of a phosphodiesterase inhibitor. Then, in A, cAMP levels were determined. In B, immunoblot analyses were performed for total and phosphorylated ERK. Data are mean \pm SD of values from 4 independent experiments in A and from 8 independent experiments in B, respectively. * p <0.05 vs. without NE treatments.

Fig. 4 NPY increased phosphorylation of ERK in stromal vascular cells of BAT in dose- and time-dependent manners. Cultured stromal vascular cells were stimulated

with increasing concentrations of NPY (0.1-100 nM) for 10 min in A and 100 nM NPY for 3-60 min in B. Immunoblot analyses for total and phosphorylated ERK were performed on 20 µg of protein of each sample, and representative blots are shown. Data are mean ± SD of values from 3 independent experiments. * p <0.05 vs. control (0 nM or 0 min).

Fig. 5 NPY increased phosphorylation of STAT3 at Ser-727, but not Tyr705, in stromal vascular cells of BAT in dose- and time-dependent manners. Cultured stromal vascular cells were stimulated with increasing concentrations of NPY (0.1-100 nM) for 10 min in A and 100 nM NPY for 3-60 min in B. Immunoblot analyses for total and phosphorylated STAT3 were performed on 20 µg of protein of each sample, and representative blots are shown. Data are mean ± SD of values from 3 independent experiments. * p <0.05 vs. control (0 nM or 0 min).

Fig. 6 PD98059 abrogated both NPY-induced phosphorylation of ERK and STAT3 at Ser727 in stromal vascular cells of BAT. Stromal vascular cells in culture were stimulated with NPY (100 nM) for 10 min, in the presence of either DMSO (-) or PD98059 (5-50 µM), an ERK kinase inhibitor. Immunoblot analyses for total and phosphorylated ERK (A) and total and phosphorylated STAT3 (B) were performed on 20 µg of protein of each sample. Representative blots are shown. Data are mean ± SD of values from 4 independent experiments. * p <0.05 vs. without NPY treatment. † p <0.05 vs. without PD98059 treatment.

Fig. 7 NPY increased *Egr1* expression in stromal vascular cells of BAT, which was

inhibited by PD98059. Stromal vascular cells in culture were stimulated with NPY (100 nM) for 1 h, in the presence of either DMSO (-) or PD98059 (+, 50 μ M). The mRNA expression of Egr-1, known as a STAT3-responsive gene, was visualized by conventional RT-PCR and quantified by real-time PCR. Data are mean \pm SD of values from 3 independent experiments. * p <0.05 vs. without NPY treatment. † p <0.05 vs. without PDD98059 treatment.

Fig. 8 NPY failed to stimulate cell growth of stromal vascular cells of BAT. Stromal vascular cells (5×10^3 cells) were cultured in 96-well plates with DMEM containing 1% FCS and increasing concentrations of NPY for 72 h. Then, the number of cells was assessed and expressed as a relative value to the control cells without NPY treatment (0 nM). Data are mean \pm SD of values from 7 independent experiments.

Fig.1

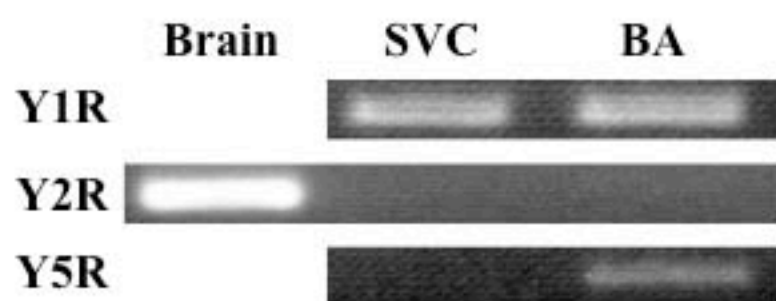


Fig. 2

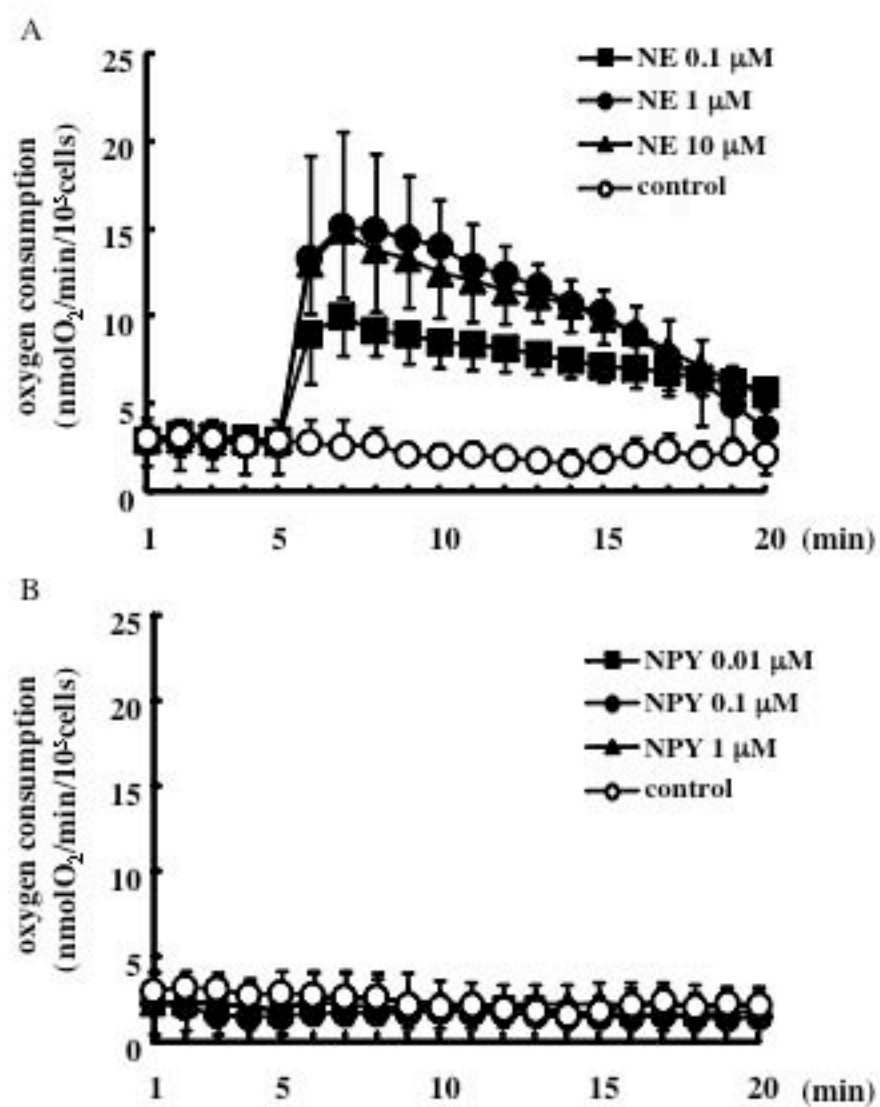


Fig.2 (continued)

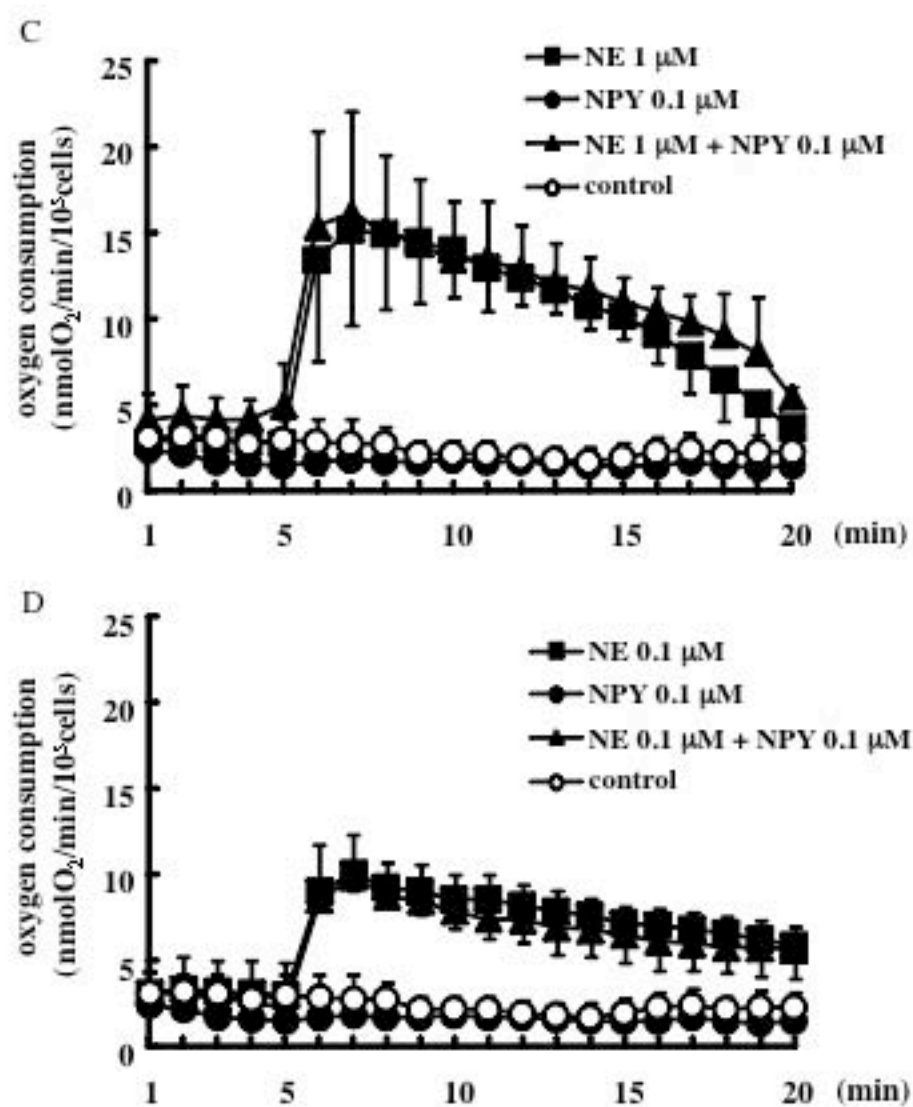


Fig. 3

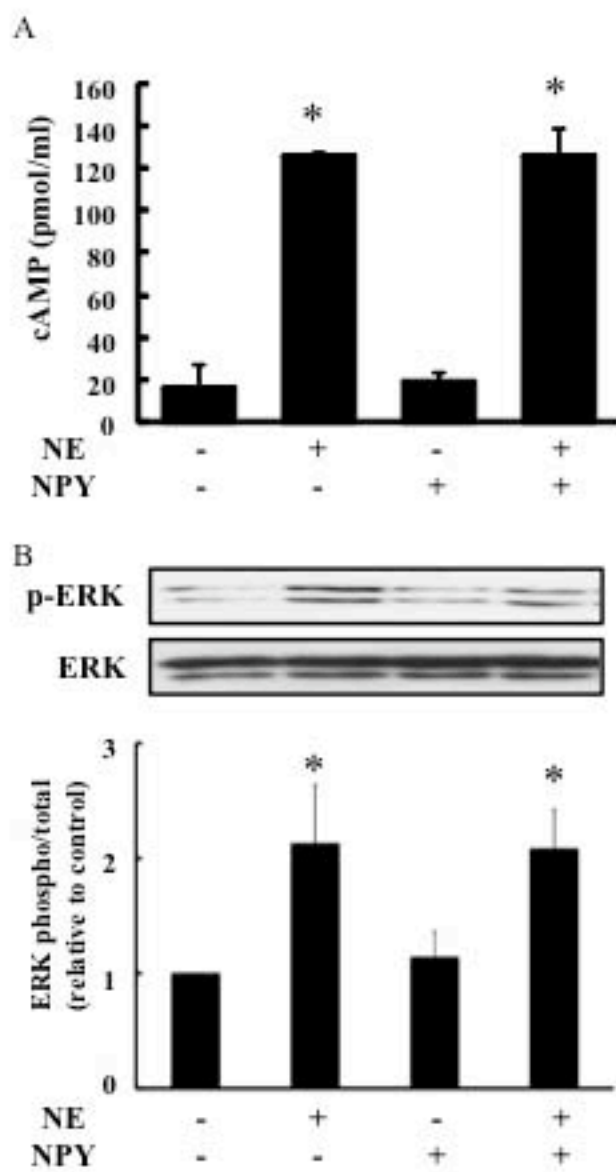


Fig.4

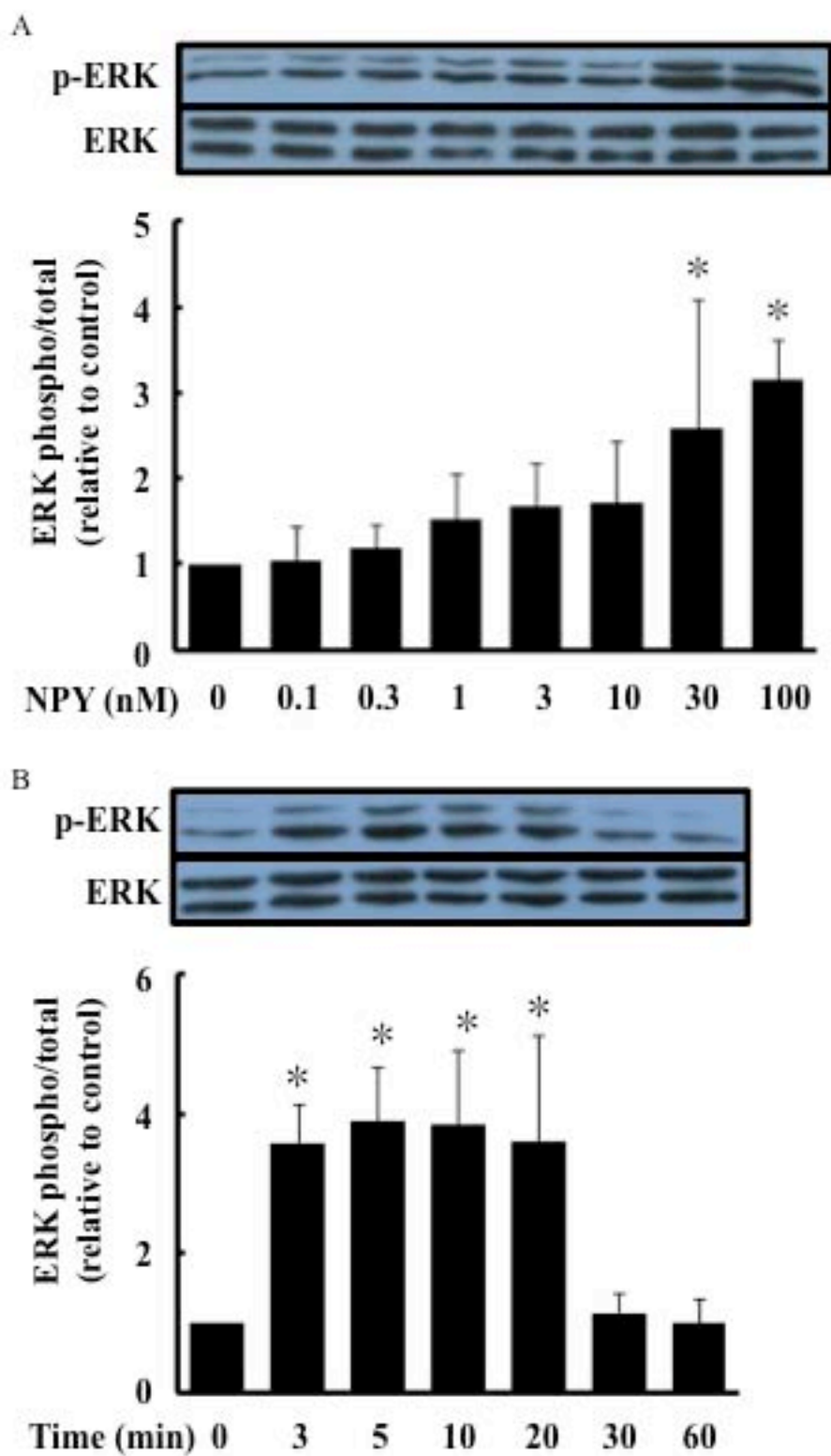


Fig.5

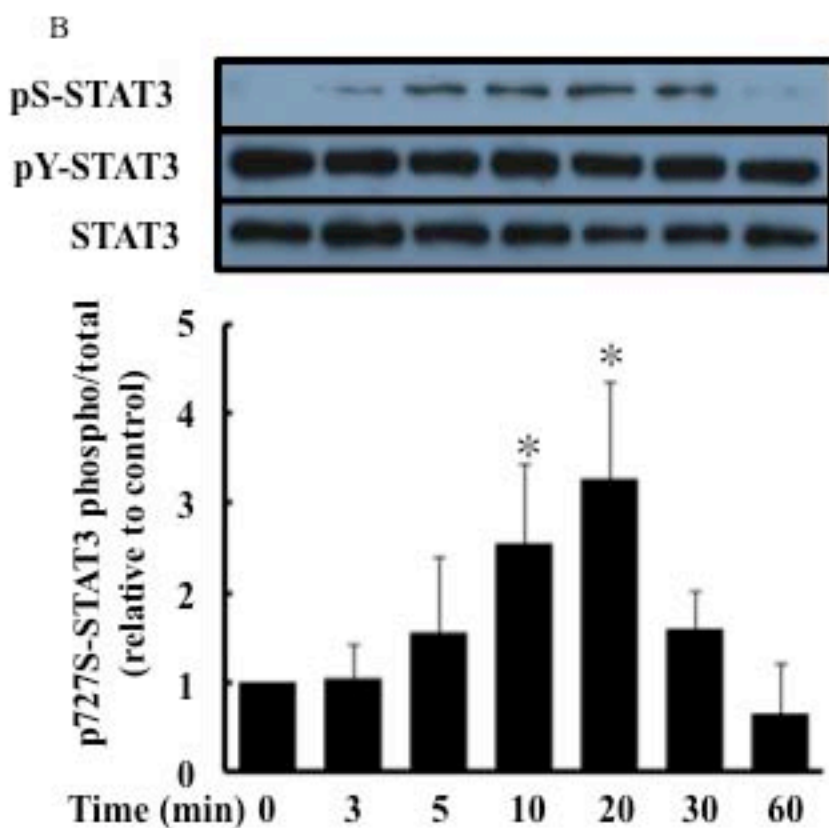
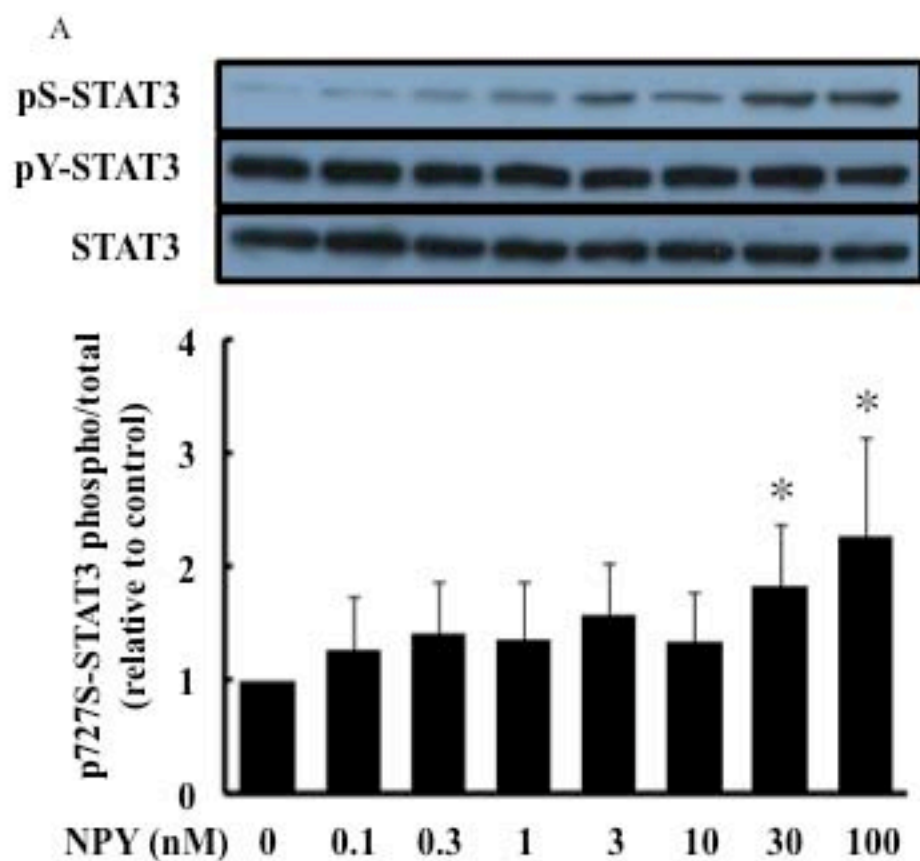


Fig. 6

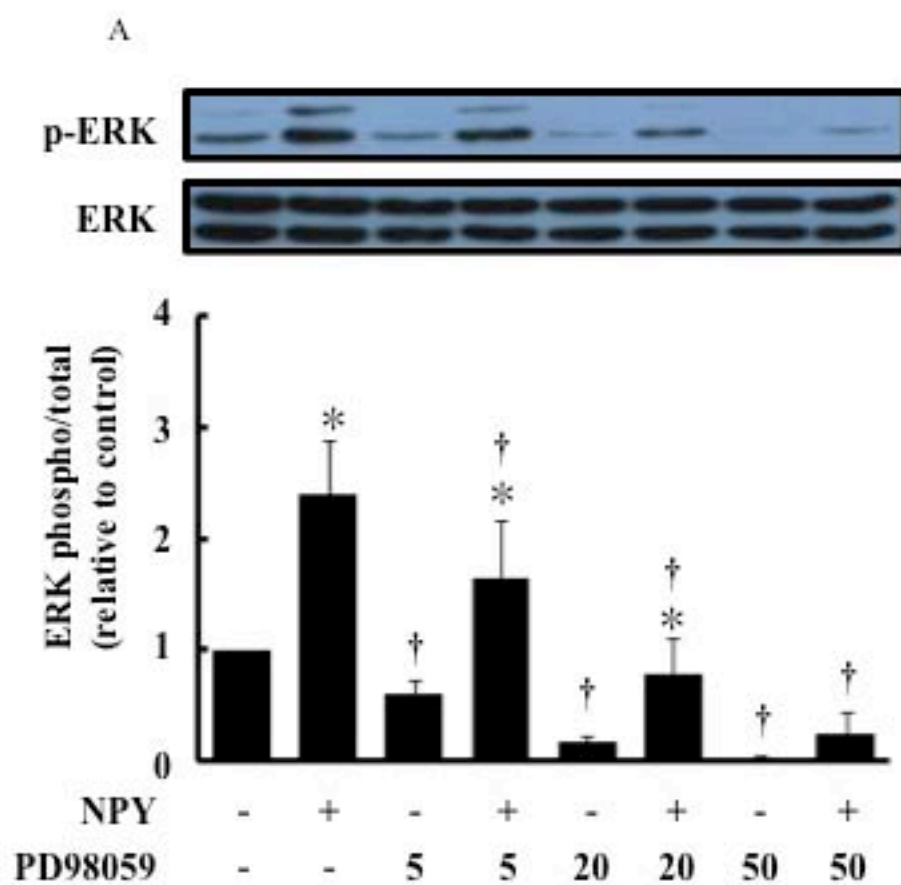


Fig. 6 (continued)

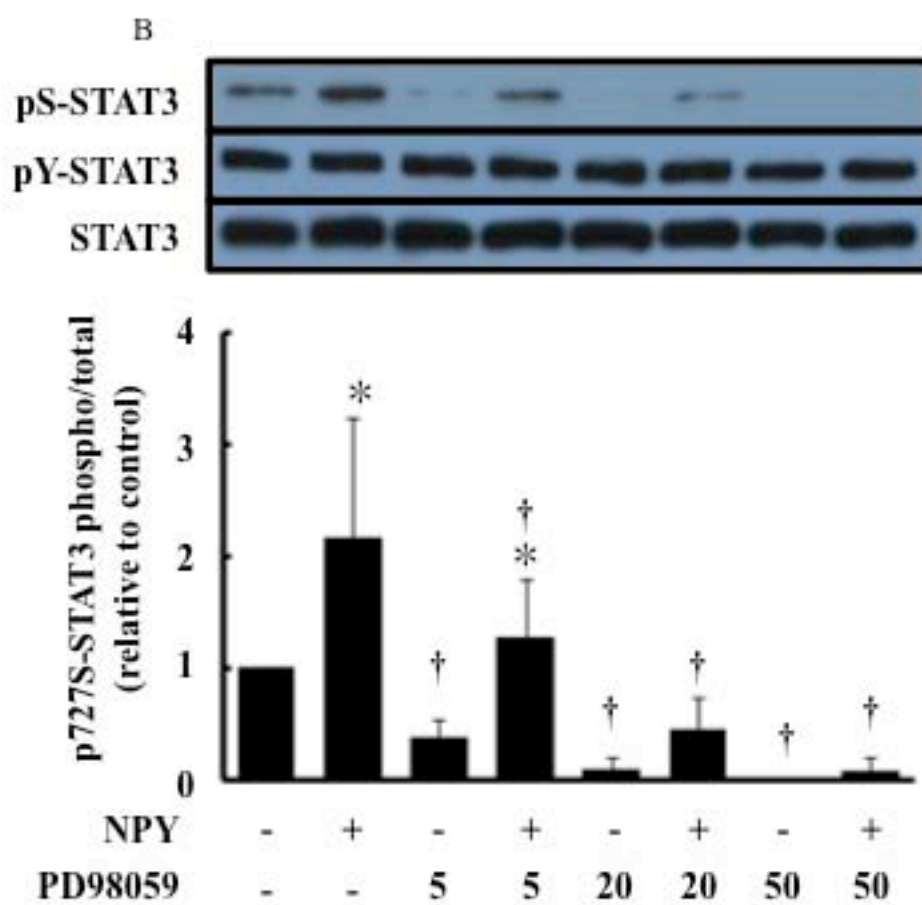


Fig. 7

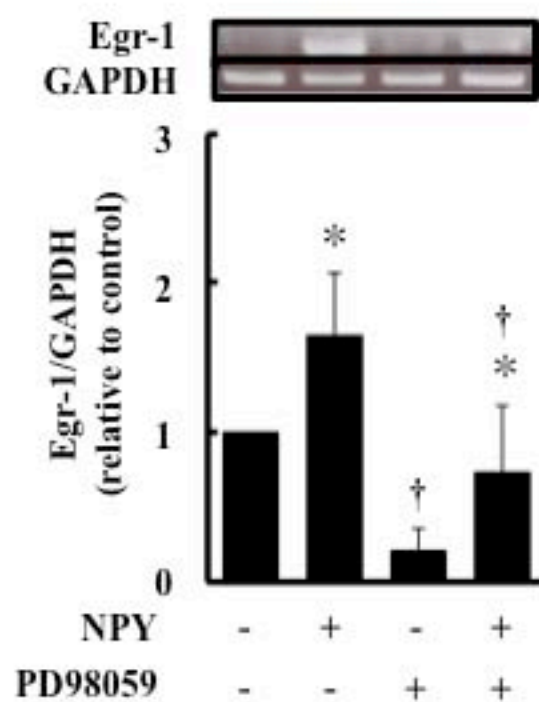


Fig.8

